

Realizing Topological Transition in a Non-Hermitian Quantum Walk with Circuit QED

Yizhou Huang,¹ Zhang-qi Yin,^{1,*} and W. L. Yang²

¹*Center for Quantum Information, Institute for Interdisciplinary Information Sciences, Tsinghua University, Beijing 100084, China*

²*State Key Laboratory of Magnetic Resonance and Atomic and Molecular Physics, Wuhan Institute of Physics and Mathematics, Chinese Academy of Sciences, Wuhan 430071, China*

We extend the non-Hermitian one-dimension quantum walk model [PRL 102, 065703 (2009)] by taking the dephasing effect into account. We prove that the feature of topological transition does not change even the dephasing between the sites within units is present. The potential experimental observation of our theoretical results in the circuit QED system consisting of superconducting qubit coupled to a superconducting resonator mode is discussed and numerically simulated. The results clearly show a topological transition in quantum walk, and display the robustness of such a system to the decay and dephasing of qubits. We also discuss how to extend model to higher dimension in the circuit QED system.

PACS numbers:

I. INTRODUCTION

As a quantum analog of the well-known classical random walk, quantum random walk serves as a fascinating framework for various quantum information processes, such as basic search [1], universal quantum computation [2], quantum measurement [3] etc. Apart from its numerous applications, quantum random walk itself also displays new traits different from its classical counterpart, such as the fast spreading of the wave function compared to a classical random walk [4], which was used for explaining the high efficiency photosynthetic energy transfer assisted by environment [5–8]. Ref. [9] considered an one-dimensional (1D) quantum random walk on a bipartite lattice, and the environment effect was included by using a non-Hermitian Hamiltonian, as done in [10]. A topological transition was found and the experimental implementation in quantum dots or cavity QED (CQED) was discussed. Later, the model was extended to multi-

dimensional systems [11].

As in Fig. 1, the quantum walk could be realized on an 1D bipartite indexed lattice where decay sites (blue) and non-decay sites (white) appear in turn. The strengths of hopping between sites are characterized by v (within the same unit) and v' (between neighboring units), and due to that, a random “walker” starting from a non-decay site of unit m_0 may end up decaying from the system from another unit m with probability P_m . Given the relative strengths of v and v' , the average displacement of a “walker” ($\sum_m m \cdot P_m - m_0$) before it decays is quantized as an integer (0 for $v' < v$ and -1 for $v' > v$) no matter what the decay co-efficient $\gamma > 0$ is. As shown in Ref. [12], such system displayed Parity-Time Symmetry [13–15]. These different displacements correspond to unbroken and broken Parity-Time Symmetry regimes and consist a topological transition. In this work we will show that such transition is robust even in the presence of dephase. Note that this idea can be experimentally realized in a CQED setting, where a qubit is coupled to one resonator mode [16, 17]. Specifically, the two states of the qubit ($|e\rangle, |g\rangle$) represent two sites of the same unit, where the higher-energy qubit state ($|e\rangle$) has decay rate γ . The cavity photon number state $|n\rangle$ represents the n -th unit. Here we suppose that the cavity decay κ is much less than qubit decay γ . Such a system could be an atom in a cavity coupled to one cavity mode. Similarly as CQED systems, a superconducting Josephson junction, which acts as a qubit, is coupled to a lumped LC oscillator in an superconducting electric circuit. Recently, circuit QED system attracts a lot of attentions, as it could be easily scaled up and controlled [18]. We will stick to the circuit QED system setup from now on. On the other hand, there were experiments realizing bipartite non-Hermitian quantum random walk in optical waveguide [19], which in essence is a classical simulation of a quantum effect. However, the non-Hermitian quantum walk in circuit QED is a fully quantum phenomenon. Another merit of circuit QED system is that

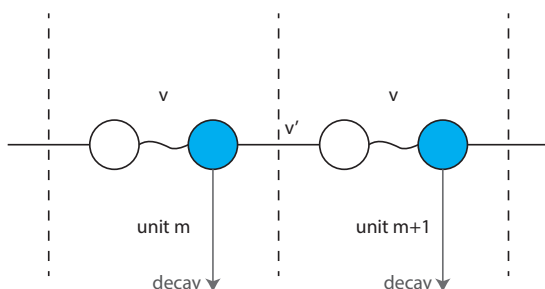


FIG. 1: (color online) Non-Hermitian quantum walk model. A particle can hope between the nearest sites with strength v (v'). Only when the particle on the blue sites, it would decay with rate γ .

*Electronic address: yinzhangqi@mail.tsinghua.edu.cn

extension to higher dimension quantum walk is relatively easy. Because a high-dimensional quantum walk can be implemented by coupling the qubit to more than one resonator mode. We will show that novel features of a quantum walk emerges with the growth of dimensionality.

In this paper, we first extend the analytical theory in [9] to accommodate the existence of dephase, and show that the qubit dephase, one of the main sources of decoherence in normal circuit QED systems, won't affect the topological structure we observed. Numerical calculations are carried out for different parameters of the system, and different factors affecting the results are considered and discussed, including the preparation of the system, the decay rate of the qubit, the detuning of the system and the effect of dephasing. We will show that such quantum walk realization is feasible in circuit QED setting, and good topological transition can be observed with modest requirement on the system parameters afore-mentioned.

II. THE CIRCUIT QED MODEL

We consider a system where a two-level qubit is coupled to a resonator field, with external microwave driving and decay of the excited state of the qubit. Such a system can be expressed in standard circuit QED Hamiltonian with a non-Hermitian decay term

$$H = g(\sigma^+ \tilde{a} + \sigma^- \tilde{a}^\dagger) + \Omega/2(\sigma^+ + \sigma^-) + \frac{1}{2}\Delta\epsilon\sigma^z - \frac{1}{2}\frac{i\gamma}{2}|e\rangle\langle e|, \quad (1)$$

where σ^z, σ^\pm are Pauli operators for the qubit, g characterizes the coupling strength, and $\tilde{a}(\tilde{a}^\dagger)$ are lowering (rising) operators on the resonator mode in a rotating frame, $\Delta\epsilon$ is (real) detuning of the system, consists of the energy differences between the two states of the qubit minus the minimum energy gap for the resonator, Ω is the strength of external drive on the atom, and γ characterizes the decay of the excited qubit state.

In usual experimental setup [20], the strength of cavity decay is at the magnitude of ~ 1 kHz or less, which is significantly smaller than other parameters in the system, such as the coupling strength g which could reach ~ 100 MHz and qubit decay γ is in the order of MHz. Therefore, we ignore the cavity decay effects. Besides, the external drive Ω is easily tunable to fulfill the topological transition conditions.

Ideally, if the system is initialized at photon number state $|N\rangle$ (which means the “walker” starts at exact site N), and stays close to N during the whole evolution process, then we can use the approximation

$$\tilde{a} \approx \sum_n \sqrt{N} |n-1\rangle\langle n|, \tilde{a}^\dagger \approx \sum_n \sqrt{N} |n\rangle\langle n-1|, \quad (2)$$

which will also be put to test in our simulation. Then, assuming $\Delta\epsilon \approx 0$, we have

$$v = \Omega/2, v' = g\sqrt{N}. \quad (3)$$

Thus, when $v' < v$ ($\frac{\Omega/2}{g} > \sqrt{N}$) the average photon number upon measurement should be N (no change), and when $v' < v$ ($\frac{\Omega/2}{g} < \sqrt{N}$) the average photon number upon measurement should be $N-1$ (change of -1).

Due to the existence of decay term $-\frac{1}{2}\frac{i\gamma}{2}|e\rangle\langle e|$ the Hamiltonian is not Hermitian. However, it satisfies the condition of Parity-Time symmetry, that is, after undergoing parity ($\hat{x} \rightarrow -\hat{x}, \hat{p} \rightarrow -\hat{p}$) and time reversal ($\hat{p} \rightarrow -\hat{p}, i \rightarrow -i$) transformation, the new Hamiltonian H' is only a constant away from the old Hamiltonian ($H' = H + cI$). And recent work [12] has proven that when we have $\frac{\Omega/2}{g} > \sqrt{N}$ the eigenvalues of the Hamiltonian are totally real, while $\frac{\Omega/2}{g} < \sqrt{N}$ there's a pair of complex energy eigenvalues, which correspond to unbroken and broken PT symmetries respectively.

III. ANALYTICAL THEORY

The analytical theory for this topological transition has been explained in detail before [9]. Here, we will improve their analytical theory to include the qubit dephase. The Lindblad master equation of the system is [21]

$$\dot{\rho}(t) = -i[H, \rho(t)] + d[\sigma^z \rho(t) \sigma^z - \rho(t)], \quad (4)$$

where d characterizes dephase rate for qubit.

If the system is pure, one could use ψ_n^A to denote the amplitude at $|g\rangle \otimes |n\rangle$ and ψ_n^B at $|e\rangle \otimes |n\rangle$. In the presence of dephase the density matrix of the system is mixed. We can similarly use density matrix as $\rho_{n_1, n_2}^{AA}(0) = \rho_{n_1, n_2}^{BA}(0) = \rho_{n_1, n_2}^{AB}(0) = 0$, $\rho_{n_1, n_2}^{BB}(0) = \delta_{n_1, 0}\delta_{n_2, 0}$, where ρ_{n_1, n_2}^{AA} is the matrix entry corresponding to $|g\rangle\langle g| \otimes |n_1\rangle\langle n_2|$ and so can be interpreted for AB , BA and BB . We have

$$\langle \Delta n \rangle = \sum_n n \cdot \left(\int_0^\infty \gamma \rho_{n, n}^{BB}(t) dt \right). \quad (5)$$

Then we translate this to momentum space by having

$$\rho_{n, n'}^{C, C'} = \frac{1}{(2\pi)^2} \oint dk \oint dk' e^{ikn} e^{-ik'n'} \rho_{k, k'}^{C, C'} \quad (6)$$

where $C, C' \in \{A, B\}$, the Hamiltonian becomes separable as for a 2×2 subspace of $|k\rangle \otimes |g/n\rangle$ we have

$$H_k = \begin{pmatrix} \epsilon_A & v_k \\ v_k^* & \epsilon_B - i\hbar\gamma/2 \end{pmatrix} \quad (7)$$

with $v_k = \frac{\Omega}{2} + g\sqrt{N}e^{-ik}$ and $\epsilon_B - \epsilon_A = \Delta\epsilon$.

Using integration by part, we have that

$$n\rho_{n, n}^{BB} = \frac{i}{(2\pi)^2} \oint dk \oint dk' e^{i(k-k')n} \partial_1 \rho_{k, k'}^{BB}. \quad (8)$$

Summing over n and integrate over time, we have

$$\langle \Delta n \rangle = i\gamma \int_0^\infty dt \oint \frac{dk}{2\pi} \partial_1 \rho_{k, k}^{BB}, \quad (9)$$

where we use $\partial_1 \rho_{k,k}^{BB}$ as a shorthand of $\frac{\partial}{\partial k'} \rho_{k',k}^{BB}|_{k'=k}$.

Now, one can define $p_k(t) := \rho_{k,k}^{AA} + \rho_{k,k}^{BB}$ as the probability that the subsystem of momentum k hasn't decay till time t , with $\partial_t p_k = -\gamma \rho_{k,k}^{BB}$. Also, one can use polar decomposition as $\rho_{k,k'}^{BB}(t) = u_{k,k'}(t) \cdot e^{i\theta_{k,k'}(t)}$. With that, one can write

$$\begin{aligned} \langle \Delta n \rangle &= \frac{i\gamma}{2\pi} \int_0^\infty dt \oint dk \left(e^{i\theta_{k,k}(t)} \partial_1 u_{k,k}(t) \right. \\ &\quad \left. + u_{k,k}(t) \cdot i \cdot e^{i\theta_{k,k}(t)} \cdot \partial_1 \theta_{k,k}(t) \right). \end{aligned} \quad (10)$$

Considering the fact that $\theta_{k,k}(t) = 0$ as the diagonal terms of a density matrix are real, and $\partial_1 u_{k,k}(t) = \partial_2 u_{k,k}(t)$, one can find that the first term $e^{i\theta_{k,k}(t)} \partial_1 u_{k,k}(t)$ induces an integration of a closed contour, and is thus zero. We can reach

$$\langle \Delta n \rangle = \frac{1}{2\pi} \int_0^\infty dt \oint dk (\partial_t p_k(t) \cdot \partial_1 \theta_{k,k}(t)). \quad (11)$$

Defining

$$I_0 = \oint \frac{dk}{2\pi} (p_k \partial_1 \theta_{k,k}(t)|_0^\infty), \quad (12)$$

we have through integration by part

$$\langle \Delta n \rangle = I_0 - \int_0^\infty \oint \frac{dk}{2\pi} p_k \partial_t \partial_1 \theta_{k,k}(t). \quad (13)$$

Given the way we conduct Fourier Transfer, we have $\rho_{k,k'} = \rho_{-k',-k}$, which means $\theta_{k,k'} = \theta_{-k',-k}$. Thus we have

$$\begin{aligned} \oint \frac{dk}{2\pi} p_k \partial_t \partial_1 \theta_{k,k}(t) &= - \oint \frac{dk}{2\pi} p_k \partial_t \partial_2 \theta_{-k,-k}(t) \\ &= \oint \frac{dk}{2\pi} p_k \partial_t \partial_2 \theta_{k,k}(t). \end{aligned} \quad (14)$$

Here we also use the fact that p_k is even function in k . Given the fact that $\partial_1 \theta_{k,k}(t) + \partial_2 \theta_{k,k}(t) = 0$, that integration yields zero, and we have $\langle \Delta n \rangle = I_0$.

Given that the system eventually decays completely, $p_k(t \rightarrow \infty) = 0$, we have

$$\langle \Delta n \rangle = - \oint \frac{dk}{2\pi} \frac{\partial \theta_{k',k}(0)}{\partial k'} \Big|_{k'=k}. \quad (15)$$

Since $\rho(0)$ is pure and diagonal in the basis of σ^z , for $\rho(\epsilon)$ consider up to the first order of ϵ , one could find that the dephase term $d(\sigma^z \rho(t) \sigma^z - \rho(t))$ doesn't affect $\rho(\epsilon)$ to the first order. Thus, by treating $\rho(\epsilon)$ as a pure state (which is similar to the case in Ref. [9]), we have

$$\langle \Delta n \rangle = - \oint \frac{dk}{2\pi} \frac{\partial \arg(-iv_k^*)}{\partial k}. \quad (16)$$

The topological structure is that, if $\Omega/2 > g\sqrt{N}$, then the integration of $-iv_k^*$ doesn't contain the axis origin and $\langle \Delta n \rangle = 0$; if $\Omega/2 < g\sqrt{N}$, then the integration of $-iv_k^*$ is an anti-clockwise contour of a circle centered at $-i\Omega/2$ and with radius $g\sqrt{N}$, which contains the axis origin, thus $\langle \Delta n \rangle = -1$.

IV. NUMERICAL RESULTS AND DISCUSSIONS

We use a simple numerical integration technique to do the simulation. A $\text{MAXN} = 320$ [22] (which is the total dimension of the Hilbert space under consideration) dimensional complex vector V (matrix, if dephase is in consideration) is used to store the state of the system. In the absence of dephase, a matrix $U = e^{-i \cdot H \cdot t}$ is computed and $U \cdot V$ simply yields the new state vector V . In the presence of qubit dephase we use Lindblad master equation (4). Integration is carried out along the way until the amplitude of V converges [23]. The time interval t shrinks by half each time and Richardson Extrapolation is carried out until the final result converges.

A first glimpse of the results are provided in Fig. 2 with $N = 100$ (which is large, as required by theory). Good topological transition is observed if the system is

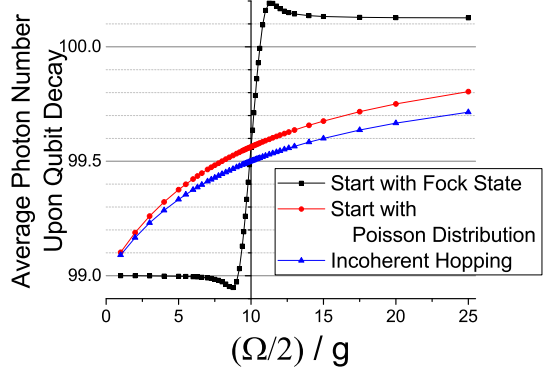
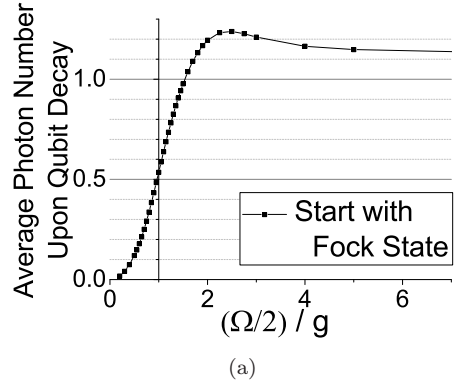


FIG. 2: (color online) Results of a basic simulation for $N=100$ with different starting conditions (Poisson / Fock), and comparison with classical incoherent hopping. The parameters are $g = 1$ (set as a benchmark), $\gamma = 4$, $\Delta\epsilon = 10^{-4}$ while $\Omega/2$ varies.

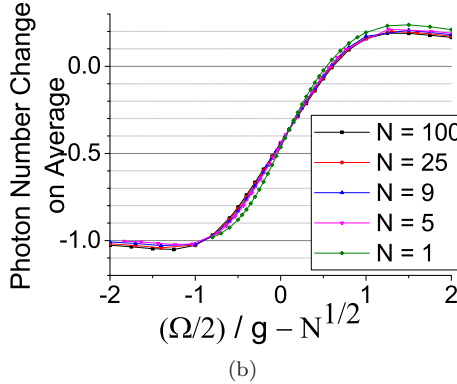
initialized in a Fock state (black).

Since large number Fock states are usually hard to prepare, we considered an alternative: coherent state (Poisson distribution), which the authors of [9] have also chosen. However, the simulation (red line in Fig. 2) turns out to be quite similar in the case of non-coherent hopping (classical walker) despite large initial N . This shows that, contrary to the Ref. [9], the Fock states are indeed necessary for testing topological transition.

Considering the fact that high energy Fock states are hard to come by, we relax the condition of $N \gg 1$ and examine some cases with small Fock numbers. An extreme case of $N = 1$ is displayed in Fig. 3(a) which still preserves the basic traits of a topological transition despite the small initial Fock number. Further investigation into the problem yields Fig. 3(b), which shows that the curve for different N 's overlap.



(a)



(b)

FIG. 3: (color online) Results of simulation for small initial N 's and comparison. The parameters in both figures are (same as Fig. 2) $g = 1, \gamma = 4, \Delta\epsilon = 10^{-4}$ while Ω varies. (a) Results of simulation with $N = 1$. (b) Displaying change in “decay energy” with respect to $\Omega/2/g - \sqrt{N}$

A. Different Decay Factors and Energy Level Differences

In this section we consider the effect of qubit decay factors γ and detuning $\Delta\epsilon$ on this experiment.

In theory [9], qubit decay factor γ only affects the (expected) evolution time, not the topological transition, so the expected result should be the same for different γ 's. We run a simulation for $N = 5$ case with identical parameters like g and $\Delta\epsilon$ for different decay factors γ 's, with result in Fig. 4. We observe that the qubit decay factor γ cannot be too small (at least $\gamma > \Omega/2, g$ should be satisfied), otherwise the photon number upon measurement would be too large.

The discrepancy between analytical theory and numerical results lies in the assumption of equation (2), which is only valid if the system stays close to photon number N throughout the whole evolution. If decay factor γ is small, the quantum walker can walk far away from the initial site, overturning that assumption. Specifically, since the system is truncated at photon number $n = 0$, the average photon number in the system would grow bigger than N , which explains the abnormal behavior for extremely small γ (green diamond) in Fig. 4.

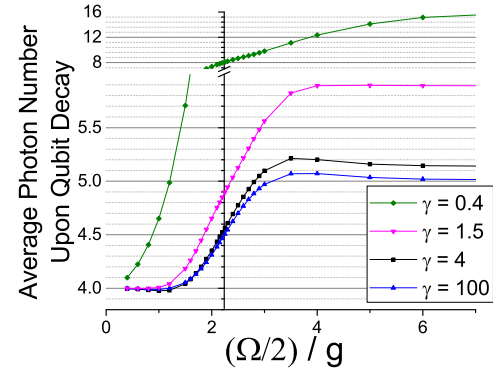


FIG. 4: (color online) Results of Simulation with different Qubit Decay Factor γ 's. Initial $N = 5$, the parameters are $g = 1, \Delta\epsilon = 10^{-4}$ while $\Omega/2$ varies.

And Fig. 5 shows the effect of detuning on this experiment. Ideally, we want $\Delta\epsilon = 0$, which is an exact match

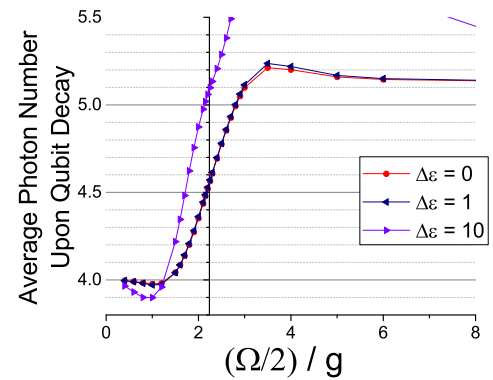


FIG. 5: (color online) Results of Simulation with different System Detuning $\Delta\epsilon$'s. Initial $N = 5$, the parameters are $g = 1, \gamma = 4$ while $\Omega/2$ varies.

to the quantum random walk scenario, although the detailed theory puts no requirement on that. Simulation shows that as long as the detuning of the system is kept small (Fig. 5 shows that $\Delta\epsilon < g, \Omega/2$ suffices), it won't have a tangible effect on the result of this experiment.

B. Dephasing Effects

Dephasing characterizes one major effect of noise on circuit QED systems, making a quantum system less “quantum” but more “classical”. Here, we consider dephase of the qubit due to external field fluctuation, which is the major source of dephase in a circuit QED system, and can be written in Lindblad master equation (4), where d characterizes the strength of such dephase. Such dephase keeps the diagonal elements of ρ , but in

addition to other standard evolution the non-diagonal elements of it shrinks exponentially by $e^{-d \cdot t}$. Here, we run a numerical simulation where qubit decay rate γ and other parameters like g , $\Delta\epsilon$ are kept identical for different qubit dephase factor d 's.

The results are in Fig. 6, which shows that the topo-

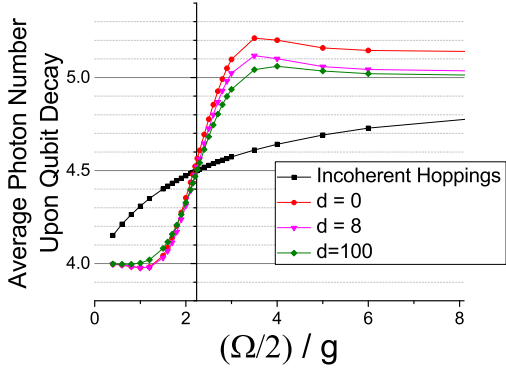


FIG. 6: (color online) Results of Simulation with different Dephase Factor d 's For the Qubit. Initial $N = 5$, the parameters are (same as Fig. 2) $g = 1$, $\gamma = 4$, $\Delta\epsilon = 10^{-4}$ while $\Omega/2$ varies.

logical transition grows less distinct as the qubit dephase factor d grows. Yet even when the dephase of the qubit is very large ($d = 100$) compared with the other elements of the system $\Omega, \gamma, g < 10$, good topological transition can still be observed, as compared to the classical incoherent hopping.

This numerical results agree with analytical theory we put forward earlier in this paper, that this topological structure is protected from the effect of dephase. No matter how much dephase we have in the system, as long as such dephase comes from external field fluctuation, and can be treated as Markovian in the timescale of other operations in the system, it won't affect experimental results.

V. 2-DIMENSIONAL QUANTUM WALK, AND ITS REALIZATION IN A CIRCUIT QED SYSTEM

As an extension, 2-dimensional quantum walk has also been investigated. Here each unit still consists of a decaying site and a non-decaying site, however, a walker could make inter-unit hopping in two dimensions, with their strengths characterized by v' and v'' each. The strength of hopping between the same unit is still v . Fig. 7 provides a sketch of the model.

The benefits of a circuit QED system is that it's relatively easy to accommodate this change by adding a second resonator mode coupled to the qubit. Like before, if one uses $|e/g\rangle \otimes |n_1\rangle \otimes |n_2\rangle$ to identify the state

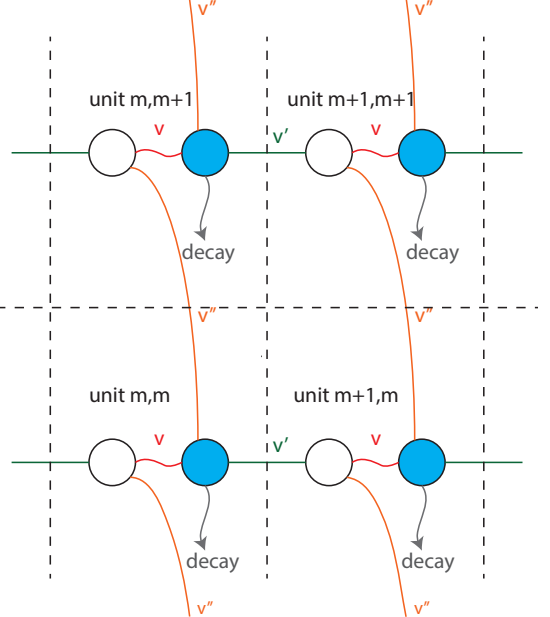


FIG. 7: (color online) Two Dimensional Quantum Walk Theory Setup. The system is similar to the one in Fig. 1, except with one more dimension. Three colors (red, orange and green) are used to distinguish different kinds of hopping.

of the system, then the Hamiltonian of the system is

$$H = g_1 (\sigma^+ \tilde{a}_1 + \sigma^- \tilde{a}_1^\dagger) + g_2 (\sigma^+ \tilde{a}_2 + \sigma^- \tilde{a}_2^\dagger) + \Omega/2(\sigma^+ + \sigma^-) + \frac{1}{2}\Delta\epsilon\sigma^z - \frac{1}{2}\frac{i\gamma}{2}|e\rangle\langle e|, \quad (17)$$

where σ 's are still Pauli operators on the qubit, and $a\tilde{a}^\dagger$'s are lowering / rising operators on the first or second resonator field in a rotating frame, $\Delta\epsilon$ is (real) detuning of the system, and γ characterizes the decay strength of the excited qubit state.

The topological structure of a 2-dimensional quantum walk is significantly different from the 1-d case as there's an intermediate area. Assuming $g_1 > g_2$, the results are

$$\langle \Delta n_1 \rangle = \begin{cases} -1 & v' > v + v'' \\ -1 + \frac{\theta_1}{\pi} & |v - v'| \leq v'' \\ 0 & v' < v - v'' \end{cases}, \quad \langle \Delta n_2 \rangle = \begin{cases} 0 & v' > v + v'' \\ -\frac{\theta_2}{\pi} & |v - v'| \leq v'' \\ 0 & v' < v - v'' \end{cases}, \quad (18)$$

with $\cos \theta_1 = \frac{N(g_1^2 - g_2^2) - \Omega^2/4}{\Omega\sqrt{N}g_2}$, $\cos \theta_2 = \frac{N(g_1^2 - g_2^2) + \Omega^2/4}{\Omega\sqrt{N}g_2}$, $v = \Omega/2$, $v' = \sqrt{N}g_1$, $v'' = \sqrt{N}g_2$ in this system. One can see a detailed theory deduction in Appendix A.

We run numerical simulations for the 2-dimensional case in a similar manner as the 1-d case, except that the tensor product of 2 vectors is stored. We truncated photon number at MAXN = 20 with hindsight knowledge from the 1-dimensional simulations. From Figure 8(a) one can see that the results of the simulation preserves the basic properties of a 2-d transition. Fig. 8(b) shows that in the 2-dimensional case, a more stringent requirement is put onto the system as a much bigger decay factor

γ is necessary to preserve the topological nature of the system compared to the one-dimensional case.

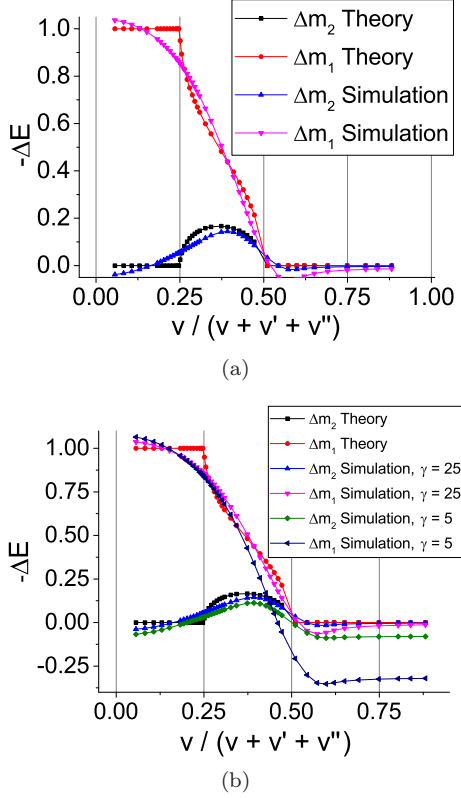


FIG. 8: (color online) Theory and simulations of 2D Hoppings. The parameters are $g_2 = 1$ (set as a benchmark), $g_1 = 2$ (to satisfy $v'/v'' = 2$) and $N = 5$ and $\Delta\epsilon = 10^{-3}$ while Ω varies. $v/(v + v' + v'') = \Omega/2/(\Omega/2 + \sqrt{N}(g_1 + g_2))$ to fit the form of independent variable. (a) Basic simulation under $\gamma = 25$ to display segmented topological transition. (b) Simulation of 2D hoppings with different decay factor γ 's.

Due to the fact that analytical theory for different dimensions follow similar integration over contours, we expect that in higher dimensional case, the topological effect would still be protected from qubit dephase.

VI. CONCLUSION

As a key element of this experimental realization, a measurement of the photon number in the cavity needs to be carried out the instance that the qubit decays. One way to implement such scheme is to prepare a low-decay qubit that's coupled to another resonator mode that has much decay. By continuous measurement of that other resonator mode [24], which provides much of the qubit decay, one can immediately sense the decay of the qubit, and thus carried out a energy measurement in the main resonator mode to retrieve photon number.

In summary, we considered the quantum walk on an one-dimensional bipartite indexed lattice, where each

unit has one decay site and one non-decay site. We have proved the topological transition in this non-Hermitian system is not affected by both the decay and the dephasing between decay and non-decay sites within units. We proposed a circuit QED implementation where a qubit is coupled to one resonator mode. We have shown that quantum random walk can be realized without too much modification to the standard JC Hamiltonian, and that topological transition could be observed to some extent even with small photon number N . We found that there was no topological transition if the systems starts in a coherent state, which is contrary to Ref. [9]. Our numerical results show that the topological structure doesn't depend on qubit dephase d , and as long as detuning $\Delta\epsilon$ of the system is kept smaller than the coupling strength g , and qubit decay is kept big (none of which are stringent), topological transition would be observable.

We would like to thank L. Sun for helpfull discussions. This work is funded by the NNSFC NO. 61435007, NO. 11574353, NO. 11274351 and NO. 11474177.

Appendix A: Analytical Theory for the Higher Dimensional

The theory for higher dimensional case without dephase has been explained in [11], which is a simple extension of the one-dimensional case, and so is the following section considering dephase.

Suppose the dimension is d . As in the one-dimensional case, one can still use $\rho_{\mathbf{n}, \mathbf{n}'}^{CC'}$ to denote the state of the system, where \mathbf{n} and \mathbf{n}' are d -dimensional vectors and $C, C' \in \{A, B\}$. The same Fourier Translation into momentum space yields that for subspace \mathbf{k} ,

$$H_{\mathbf{k}} = \begin{pmatrix} \epsilon_A & \mathbf{A}_{\mathbf{k}} \\ \mathbf{A}_{\mathbf{k}}^* & \epsilon_B - i\hbar\gamma/2 \end{pmatrix} \quad (A1)$$

with $\mathbf{A}_{\mathbf{k}} = \frac{\Omega}{2} + \sum_{\alpha=1}^d g^{(\alpha)} \sqrt{N} e^{-ik_{\alpha}}$. Defining $p_{\mathbf{k}}(t)$ in the same way as

$$p_{\mathbf{k}} = \rho_{\mathbf{k}, \mathbf{k}}^{AA} + \rho_{\mathbf{k}, \mathbf{k}}^{BB} \quad (A2)$$

and with $\partial_t p_{\mathbf{k}} = -\gamma \psi_{\mathbf{k}, \mathbf{k}}^{BB}(t)$ and integrate by part, one can reach

$$\langle \Delta n_{\alpha} \rangle = \oint \frac{d^{d-1}k}{(2\pi)^{d-1}} \left\{ i\gamma \int_0^{\infty} dt \oint \frac{dk_{\alpha}}{2\pi} \partial_{k_{\alpha}, 1} \rho_{\mathbf{k}, \mathbf{k}}^{BB} \right\}, \quad (A3)$$

while the shorthand $\partial_{k_{\alpha}, 1}$ means taking partial derivative only on the α -th component of \mathbf{k} , and only on the first \mathbf{k} in the density matrix. It's not hard to see that the expression inside the brace is exactly as equation (9) and thus is either 0 or 1, no matter what dephasing factors we have.

Now, if one come back to the definition of $\mathbf{A}_{\mathbf{k}} = \frac{\Omega}{2} + \sum_{\alpha=1}^d g^{(\alpha)} \sqrt{N} e^{-ik_{\alpha}}$, one way to understand equation (A3) is to first fix $d-1$ angles $k_{\beta \neq \alpha}$, then see whether the integration of k_{α} from 0 to 2π would case the angle of $\mathbf{A}_{\mathbf{k}}$

to also shift 2π , and integration over those $d - 1$ angles. During the integration of the other $d - 1$ angles, some traits of topology might be lost, like the middle area of

Fig. 8(a), and some may remain, like the two sides of Fig. 8(a).

[1] M. Szegedy, Quantum Speed-Up of Markov Chain Based Algorithms, in *Proceedings of the 45th IEEE Symposium on Foundations of Computer Science* (IEEE, New York, 2004), pp. 32-41.

[2] A. M. Childs, Universal computation by quantum walk, *Phys. Rev. Lett.* **102**, 180501 (2009).

[3] Z. H. Bian, J. Li, H. Qin, X. Zhan, R. Zhang, B. C. Sanders, and P. Xue, Realization of Single-Qubit Positive-Operator-Valued Measurement via a One-Dimensional Photonic Quantum Walks, *Phys. Rev. Lett.* **114**, 203602 (2015).

[4] A. Ambainis, E. Bach, A. Nayak, A. Vishwanath, J. Watrous, One-dimensional quantum random walk, in *Proceedings of the 33rd Annual ACM Symposium on Theory of Computing* (ACM Press, New York, 2001), pp. 37-49.

[5] Gregory S. Engel *et al*, Evidence for wavelike energy transfer through quantum coherence in photosynthetic systems. *Nature (London)* **446**, 782 (2007).

[6] M. Mohseni, *et al*, Environment-assisted quantum walks in photosynthetic energy transfer, *J. Chem. Phys.* **129** 174106 (2008).

[7] Qing Ai, Tzu-Chi Yen, Bih-Yaw Jin, and Yuan-Chung Cheng, Clustered Geometries Exploiting Quantum Coherence Effects for Efficient Energy Transfer in Light Harvesting, *J. Phys. Chem. Lett.* **4**, 2577 (2013).

[8] Qing Ai, Yuan-Jia Fan, Bih-Yaw Jin and Yuan-Chung Cheng, An efficient quantum jump method for coherent energy transfer dynamics in photosynthetic systems under the influence of laser fields, *New J. Phys.* **16**, 053033 (2014).

[9] M. S. Rudner and L. S. Levitov, Topological Transition in a Non-Hermitian Quantum Walk, *Phys. Rev. Lett.* **102**, 065703 (2009).

[10] Carl M. Bender, Making Sense of Non-Hermitian Hamiltonians, *Rept. Prog. Phys.* **70**, 947 (2007).

[11] M. S. Rudner and L. S. Levitov, Phase transitions in dissipative quantum transport and mesoscopic nuclear spin pumping, *Phys. Rev. B* **82**, 155418 (2010).

[12] S. Longshi, Convective and absolute PT-symmetry breaking in tight-binding lattices, *Phys. Rev. A* **88**, 052102 (2013).

[13] C. M. Bender and S. Boettcher, Real Spectra in Non-Hermitian Hamiltonians Having PT Symmetry, *Phys. Rev. Lett.* **80**, 5243 (1998).

[14] C. E. Rüter *et al*, Observation of parity-time symmetry in optics, *Nature Physics* **6**, 192 (2010).

[15] L Chang, X Jiang, S Hua, C Yang, J Wen, L Jiang, G Li, G Wang, M Xiao, Parity-time symmetry and variable optical isolation in active-passive-coupled microresonators, *Nature Photonics* **8**, 524 (2014).

[16] Herbert Walther, Benjamin T H Varcoe, Berthold-Georg Englert and Thomas Becker, Cavity quantum electrodynamics, *Rep. Prog. Phys.* **69**, 1325 (2006).

[17] Zhang-qi Yin and Fu-li Li, Multiatom and resonant interaction scheme for quantum state transfer and logical gates between two remote cavities via an optical fiber, *Phys. Rev. A* **75**, 012324 (2007).

[18] A. Blais, J. Gambetta, A. Wallraff, D. I. Schuster, S. M. Girvin, M. H. Devoret, and R. J. Schoelkopf, Quantum-information processing with circuit quantum electrodynamics, *Phys. Rev. A* **75**, 032329 (2007).

[19] J. M. Zeuner, M. C. Rechtsman, Y. Plotnik, Observation of a topological transition in the bulk of a non-Hermitian system, *Phys. Rev. Lett.* **115**, 040402 (2015).

[20] M. Reagor, H. Paik, G. Catelani, L. Sun, C. Axline, E. Holland, I. M. Pop, N. A. Masluk, T. Brecht, L. Frunzio, M. H. Devoret, L. Glazman, and R. J. Schoelkopf, Reaching 10 ms single photon lifetimes for superconducting aluminum cavities, *Appl. Phys. Lett.* **102**, 192604 (2013).

[21] H. M. Wiseman and G. J. Milburn, *Quantum Measurement and Control*. (Cambridge University Press, Cambridge, England, 2009).

[22] Although with hindsight we only need the dimension of Hilbert space for the resonator to be $2N$, which means $\text{MAXN} \sim 4N$ is simply enough. Choosing such a large number is to make sure that we don't need to change the configuration of the system for different initial Fock state numbers like $N = 1$ and $N = 100$.

[23] Due to the existence of “dark state” for finite systems, that amplitude won't go to exactly zero.

[24] L. Sun, A. Petrenko, Z. Leghtas, B. Vlastakis, G. Kirchmair, K. M. Sliwa, A. Narla, M. Hatridge, S. Shankar, J. Blumoff, L. Frunzio, M. Mirrahimi, M. H. Devoret, and R. J. Schoelkopf, Tracking Photon Jumps with Repeated Quantum Non-Demolition Parity Measurements, *Nature (London)* **511**, 444 (2014).